Exploring Residual and Spatial Consistency for Object Detection

Hao Wang, Ya Zhang and Zhe Xu
Institute of Image Communication and Information Processing
Shanghai Jiao Tong University, Shanghai, China

Keywords: Visual Object Detection, Wide Baseline Matching, Local Image Feature, Spatial Consistency.

Abstract: Local image features show a high degree of repeatability, while their local appearance usually does not bring enough discriminative pattern to obtain a reliable matching. In this paper, we present a new object matching algorithm based on a novel robust estimation of residual consensus and flexible spatial consistency filter. We evaluate the similarity between different homography model via two-parameter integrated Weibull distribution and inlier probabilities estimates, which can select uncontaminated model to help eliminating outliers. Spatial consistency test was encoded by the geometric relationships of domain knowledge in two directions, which is invariant to scale, rotation, and translation especially robust to the flipped image. Experiment results on nature images with clutter background demonstrate our method effectiveness and robustness.

1 INTRODUCTION

With the increasing popularity of image applications on internet such as Google Image and Flickr, considerable attention has been directed to image detection and classification in multimedia research communities. However, accurate object recognition remains a challenging problem, because the target object may be small in size with cluttered background, or it is significantly different from the query image in color, scale, and orientation.

Among existing methods, the bag-of-features model (Sivic and Zisserman, 2003; Lazebnik et al., 2006) has been a popular technique because of its simplicity and effectiveness. This method quantizes local image descriptors into distinct visual words for scalable image indexing and searching. With the inverted index of visual words, one not only avoids storing and comparing high dimensional local descriptors, but also reduces the number of candidate images because only images sharing common words with the query image are considered. To improve the precision of the matching, a visual word may be augmented with compact information from its original local descriptor, including a Hamming code (Jegou et al., 2008), descriptor scale and angle, and the distance (in descriptor space) to its neighboring visual words.

Geometric verification such as RANSAC is a crucial step after retrieval from the inverted index. Many extensions of RANSAC have been proposed in order to improve the accuracy of the matching. Multi-GS (Chin et al., 2010) accelerates hypothesis sampling by guiding it with information derived from residual sorting. The LO-RANSAC (Chum et al., 2003) method introduces an inner RANSAC loop into the main RANSAC algorithm such that hypotheses may be generated from the set of inliers. Guided-MLESAC (Tordoff and Murray, 2005) and PROSAC (Chum and Matas, 2005) focus on sampling more confident keypoint matches. The above two methods are essentially guided only by the prior inlier probabilities and do not conduct conditional sampling to further improve efficiency. GroupSAC (Ni et al., 2009) focuses on sampling groups of data obtained using image segmentation. SCRAMSAC (Sattler et al., 2009) introduces a spatial filtering step such that matches with similar local geometry are considered. ARRSAC (Raguram et al., 2008) performs a partially breadth-first verification such that the number of hypotheses may be modified according to the inlier ratio estimation while still bounding the runtime.

In recent years, spatial context have been proven to be useful for enhancing the discriminative power of individual local features. Features that are close to each other are grouped to form a visual phrase. Visual phrase is formed by two different methods. The first type of methods mainly relies on object segmentation or region detection, which finds spatial context of object locating area by detecting contour (Russell et al., 2006; Wu et al., 2009). An example of such meth-

Wang H., Zhang Y. and Xu Z..
Exploring Residual and Spatial Consistency for Object Detection.
DOI: 10.5220/0004746801910197
In *Proceedings of the 9th International Conference on Computer Vision Theory and Applications* (VISAPP-2014), pages 191-197
ISBN: 978-989-758-004-8

ods is bundled-feature which groups features in local MSER regions described by SIFT into a local group to increase the discriminative power of local features (Zhang et al., 2011). However, object need to be segmented accurately. Otherwise the visual phrase will be far away from the correct area. The second type of methods selects the visual phrase at a fixed area, such as geometry-preserving visual phrases that capture long-range spatial layouts of the words (Sivic and Zisserman, 2009). They were generating a higher-level lexicon, i.e. visual phrase lexicon, where a visual phrase is a meaningful spatially co-occurrent pattern of visual words (Jiang et al., 2011; Li et al., 2011). In (Lowe, 2004), local spatial consistency from some spatial nearest neighbors is used to filter false visual-word matches.

In this work, we propose a novel robust estimation of residual consensus and flexible spatial consistency filter for object matching. Specifically, we evaluate the similar structure from different homography models in two aspects. Firstly, We extend RANSAC to model residuals distribution using two-parameter integrated Weibull which is between a power-law and a Gaussian distribution. Secondly, we calculate the normalized overlap of sorted residuals obtained from hypothesis generation. For spatial consistency filter, previous literatures usually describe the relative spatial positions between each feature pair along the horizontal (X-axis) and vertical (Y-axis) directions or measuring angles only in one direction. However, we measure spatial consistency using geometric relationships of globally point distribution in both clockwise and counterclockwise, which is invariant to scale, rotation, and translation especially robust to flipped image.

2 RESIDUAL AND SPATIAL CONSISTENCY

The SIFT feature is one of the most robust and distinctive features (Kalantidis et al., 2011). SIFT feature descriptor is invariant to uniform scaling orientation, and partially invariant to affine distortion and illumination changes. Local interest points are extracted by DOG detector and described by 128-dimensional SIFT descriptor. A bag of visual words (BOW) is obtained by quantizing high-dimensional local image descriptors through clustering. An inverted index structure is used for retrieval and each visual word has an entry in the index that contains the list of images in which the visual word occurs. Additionally, the tf-idf weight is used to distinguish different matched features. However, this structure ignores geometric relationships among visual words due to quantization. Geometric verification such as RANSAC becomes an important post-processing step for getting reasonable retrieval precision, especially for distorted images. Given a set of tentative correspondences, a minimal subset of size m is randomly sampled to hypothesize a geometric model. Then the model is verified by the remaining correspondences. This process is iterated until a termination is met. Despite the effectiveness of RANSAC, false matching might still appear in a real application. An extension of the RANSAC is proposed by adding an optimization procedure to solve this problem. We compute the similarity between different homography model via residual ordering distribution, which can select uncontaminated model to help eliminating outliers. Spatial consistency test was encoded by the geometric relationships of domain knowledge in both clockwise and counterclockwise, which is measured by relative orientation and distance order. The use of spatial configuration of local features aims at reducing the number of mismatches in the correspondence set.

2.1 Residual Consensus

Residual ordering distribution is useful for distinguishing between contaminated models and uncontaminated models. Naturally, residual errors obtained from uncontaminated models are approximate similar with each other. Thus, potential patterns can be discovered by evaluating the similarity between these structures to help finding the optimal models.

Formally, given a set of N input data. Under the hypothesize-and-verify framework, a model is fitted by a minimal sample. Let $R^i = \{r_1^i, r_2^i, ..., r_N^i\}$ be absolute residuals corresponding to the input data. We then find the permutation $S^i = \{\lambda_1^i, \lambda_2^i, ...\lambda_N^i\}$ such that the residuals are sorted in increasing order. We define the intersection set $\Theta_n^{i,j}$ as,

$$\Theta_n^{i,j} = S_{1:n}^i \bigcap S_{1:n}^j, \tag{1}$$

where $S_{1:n}^i$ denote the subset containing the first n points of S^i and $S_{1:n}^i \bigcap S_{1:n}^j$ finds the number of overlap elements from $S_{1:n}^i$ and $S_{1:n}^j$. We also give the normalized overlap $\theta_n^{i,j}$.

$$\theta_n^{i,j} = \frac{1}{n}|\Theta_n^{i,j}|, \tag{2}$$

Intuitively, Similar models should have the most overlap of small value residuals. To verify this method for distinguish uncontaminated and contaminated models, an example is shown to illustrates this intuition explained. In details, we generate 400 homography hypotheses on the real images and select the uncontaminated models to compare with the random models. Fig.1(a) plots the normalized overlap $\theta_n^{i,j}$ of sorted residuals from uncontaminated models and random models, respectively. Fig.1(b) shows a block diagonal pattern of $\theta_n^{i,j}(1 \leq i,j \leq 400)$, in which, the points are scattered according to their structure membership. The results show that, the values for an inlier concentrate mostly on other inliers from the same distribution, while for a outlier the value are generally low and appear to be randomly distributed.

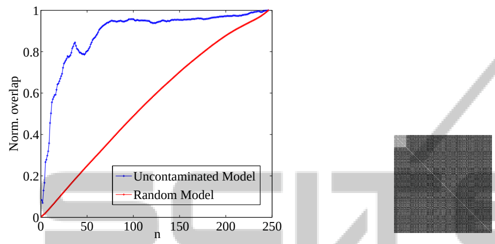

(a) (b)

Figure 1: (a) Normalized overlap vs. subset size n for uncontaminated models and random models. (b) The corresponding matrix of size 400*400 with subset is set to 80.

We use a statistical model as an another means to characterize the qualitive differences between models. By observing the data, the distribution of residuals is usually between a power-law and a Gaussian distribution, can be well modeled by a two-parameter integrated Weibull distribution,

$$p(x) = \frac{\gamma}{2\gamma^{\frac{1}{\gamma}}\beta\Gamma(\frac{1}{\gamma})} exp\{-\frac{1}{\gamma}|\frac{x}{\beta}|^{\gamma}\}, \tag{3}$$

where x is the residuals of geometric model. $\gamma > 0$ denotes the peakness of the distribution. $\beta > 0$ represents the scale parameter of the distribution. $\Gamma(x)$ is the complete Gamma function.

$$\Gamma(x) = \int_0^{\infty} t^{x-1} exp(-t) dt, \tag{4}$$

Given the observed data $X = x_1, x_2, \ldots x_n$. The best fit is obtained when model parameters maximize the log-likelihood function, in which case their respective derivatives should equal zero.

$$\frac{\partial}{\partial\beta} \ln L_{iw}(\beta,\gamma|X) = -\frac{1}{\beta} + \frac{1}{\beta}\sum_{i=1}^{n}|\frac{x_i}{\beta}|^{\gamma} = 0, \tag{5}$$

$$\begin{aligned}\frac{\partial}{\partial\gamma} \ln L_{iw}(\beta,\gamma|X) = \frac{1}{\gamma^2}(\gamma - 1 + \Psi(\frac{1}{\gamma}) +& \\ \ln(\gamma) + \sum_{i=1}^{n}|\frac{x_i}{\beta}|^{\gamma}),&\end{aligned} \tag{6}$$

$$\Psi(\gamma) = \frac{d}{d\gamma}\ln\Gamma(\gamma) = \frac{\frac{d}{d\gamma}\Gamma(\gamma)}{\Gamma(\gamma)}, \tag{7}$$

The parameter is obtained by eliminating from Eq.(6):

$$\begin{aligned} f(\gamma,X) = -\frac{1}{\gamma}\sum_{i=1}^{n}\frac{|x_i|^{\gamma}}{\sum_{i=1}^{n}|x_i|^{\gamma}}\ln\frac{|x_i|^{\gamma}}{\sum_{i=1}^{n}|x_i|^{\gamma}}& \\ +1+\frac{1}{\gamma}\ln(\gamma)+\frac{1}{\gamma}\Psi(\frac{1}{\gamma}) = 0.&\end{aligned} \tag{8}$$

Eq.(6) is solved using standard iterative procedures, for example, the Newton-Raphson. Fig.2(a) displays the fitting result using an integrated Weibull distribution. The residual is subtracted by median because we want the peak of probability density is located on where residual equal zero. As in Fig.2(b), we can see that the two parameters of models build up a 2-D map and the most uncontaminated models come from the intensive area. Therefore, we can use this property to capture uncontaminated models. Given discrete data points from 2-D map, the center of the intensive area is located using mean-shift method (Comaniciu and Meer, 2002). Here, the mean-shift path toward the mode follows a smooth trajectory, and the angle between two consecutive vectors being always less than 90 degrees. The search procedure can be interpreted as kernel density estimation for the position of the model distribution points. Moreover, we define an elliptical area lying on the center of the 2-D map, such that, the major axis l_1 parallel to scale axis and minor axis l_2 parallel to shape axis. In this case, the models within the elliptical area are kept for spatial consistency test and unpromising hypotheses can be quickly filtered out .

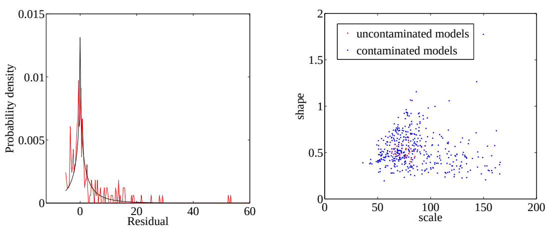

(a) (b)

Figure 2: (a) Residual distribution is fitted by an integrated Weibull model. (b) The parameter map of uncontaminated models and contaminated models.

2.2 Spatial Consistency Analysis

Given an image I, we extract a set of visual words $U(I) = \{u_i\}$ with center coordinates (x_i, y_i) and $V(I) = \{v_j\}$ is another visual word. In an image pair

(I_1, I_2), all the point correspondences are established by visual words. Thus, we obtain a correspondence set C,

$$C = \{(u_i, v_j) | u_i \in U \wedge v_j \in V\}. \tag{9}$$

We define a matching score $M(I_1, I_2)$, which consists of a membership term $M_m(I_1, I_2)$ and a geometric $M_g(I_1, I_2)$.

$$M(U,V) = M_m(U,V) + \lambda M_g(U,V), \tag{10}$$

where λ is a weighting parameter. For membership term, we compute inlier scores to define the membership term $M_m(U,V)$.

Our geometric term performs a weak geometric verification between training image I_1 and query image I_2 using relative ordering, and we incorporate orientation configuration into distance configuration. In detail, the minimal value of two kinds of configuration is the final value,

$$M_g(U,V) = min(M_{g1}(U,V), M_{g2}(U,V)), \tag{11}$$

where, $M_{g1}(U,V)$ is orientation configuration term and $M_{g2}(U,V)$ is distance configuration term. As in Fig.3, the centroid of all the features is located as a reference point. Starting from zero degree, the whole visual words position is scanned clockwise. As the angle increases, each visual word is assigned a number with ascending order. Note that the visual word from testing image has the same number as training one if they are the matching pair. The inconsistency is accumulated by the difference of neighbor number between training image and testing image,

$$M_{g1}^{D}(U,V) = -\sum_{i} \delta(O_v[u_i] > O_v[u_{i+1}]), \tag{12}$$

where D is a pre-defined geometric sorting order, and $\delta(O_v[u_i] > O_v[u_{i+1}])$ is an indicator function that measures the consistency between the order $i < i+1$ (before matching) and the order $O_v[u_i] > O_v[u_{i+1}]$ (after matching). In other words, we penalize geometric inconsistency of the visual word matching between two images and put a weight to inconsistency avoid for weak discrimination by small difference. In order to match flipped image, the minimal inconsistency is set as final scores from clockwise and counterclockwise image scan,

$$M_g(U,V) = min(M_g^{C}(U,V), M_g^{A}(U,V)), \tag{13}$$

where $M_g^{C}(U,V)$ is computed by a geometric verification via clockwise, and $M_g^{A}(U,V)$ by a counterclockwise geometric verification. For spatial consistency filter with distance, the only difference between orientation is that we compare the distance from reference point to the position of visual words.

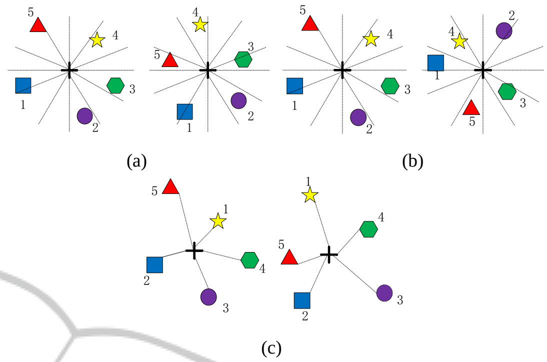

Figure 3: The ordering constraint for local features. (a) Correct matches preserve the relative orientation orders; (b) Wrong matches results in inconsistent relative orientation orders; (c) Wrong matches results in inconsistent relative distance orders.

2.3 Algorithm

Consider the residual consensus aforementioned, a statistical rest that evaluates the similarity between distributions can give the optimal homography model. Specifically, we first measure the fraction of models by Weibull distribution intensive area which is located using mean-shift method. Then we restrict all further processing to correspondences where this fraction surpasses a threshold T by inlier probabilities estimates, resulting in a reduced set of models. our approach combines the robust estimation of residual consensus and spatial consistency filter in a unified framework. The details of algorithm are shown in Algorithm 1.

Generally, image retrieval system uses criteria whether the absolute matching number exceeds a certain threshold to decide the final matching results. However, taking into account the different complexity of the images and different number of features, which lead to more correspondence generating in images with large number features. In that case, even if the query image does not have the object, the features of the object still have high probabilities to match the other parts of the image. In our approach, we use the total number of features as penalty factor to eliminate this problem. Note that the importance of inliers is different because of residuals of geometric model have diverse values. The residual with small values is more important for correspondence selection, because they have high probabilities to become true inliers. We follow MLESAC(Maximum Likelihood SAC) (Torr and Zisserman, 2000) to define the

Algorithm 1: Residual and spatial consistency.

1. Hypothesis generation
$k = 0$
while $k < k_{max}$ **do**
  Randomly sample minimal subset of m points.
  Estimate model parameters θ_k.
end while
2. Residual consensus
Sort residuals, store sorted index S_i and residual errors
for all models S^i in $\{M_1, M_2, ...M_{i-1}\}$ **do**
  Fit integrated Weibull distribution to sorted residuals.
  The most intensive area S_* is located using mean-shift method.
  Store models come from this area.
  Compute intersection $\Theta_n^{i,j}$ for M_i and M_j, and normalize to $\theta_n^{i,j}$.
  if $\theta_n^{i,j} > T$ for some n **then**
    Store K uncontaminated models and find the model with large number inliers.
  end if
end for
3. Spatial Consistency
Gain orientation and distance between visual word via position and centroid.
Compute inconsistency $M_g(U,V)$ using different permutation.

loss function. It models inliers error as unbiased Gaussian distribution and outlier error as uniform distribution.

3 EXPERIMENTAL RESULTS

In this section, experiments were conducted to demonstrate the effectiveness of the proposed residual and spatial consistency method on real image datasets. Yannis et al. [16] built the FlickrLogos dataset by downloading real-world images from Flickr containing 27 logos covering various aspects of life. The 27 logo classes is Adidas, Apple, BMW, Citroen, Coca-Cola, DHL, Fedex, Ferrari, Ford, Google, Heineken, HP, Intel, McDonalds, Mini, Nbc, Nike, Pepsi, Porsche, Puma, RedBull, Sprite, Starbucks, Texaco, Unicef, Vodafone, and Yahoo. The dataset selected 40 images per class from Flickr, and every selected image include at least one instance of the brands logo. All 1080 images were annotated with bounding boxes. The annotated logo was partitioned into 2 subsets: The training set has 30 randomly selected images from the 40 images per brand, and the rest were the test set. To further verify the scalability and effectiveness of our approach, we add 500 crawled Flickr images with noting logos and 230 with logos to the test set.

Baseline. We use Trademark Matching (Bagdanov et al., 2007) approach with RANSAC as the baseline approach, which is denoted as "RANSAC". The method is a compact representation of trademarks and video frame content based on SIFT feature points, which is state-of-the-art logo detection methods, and has been used in commercial application. In the paper, a visual vocabulary of 2M visual words is adopted. In fact, we have experimented with different visual codebook sizes, and have found the 2M vocabularies yield the best overall performance for the baseline.

Comparisons. Another two compared algorithms are improved versions of baseline by adding different geometry consistency. The first one is Hamming Embedding [3] by adding a hamming code to filter out matched features that have the same number of quantized visual words but have a large hamming distance from the query feature. We denote this method as "HE." The second one is accelerate hypothesis sampling by guiding it with information derived from residual sorting [6], which is denoted as "Multisac".

In this paper, we set a fraction of inliers T to 0.95 in Residual consensus evaluation. For pairs of uncontaminated models, we found that when subset n close to the true inlier ratio, $\theta_n^{i,j}$ is approaching T. For parameter of elliptical area, we set the value of l_1 and l_2 to 40 and 0.25. We look for K good models to provide robustness structure. In our experiments, setting K = 3 was sufficient in practice. We empirically examine the ratio of optimal RANSAC score and geometric inconsistency. The parameter is set in the range of $\lambda = [0, 0.5, ..., 2.5]$. For each varying of λ, we run the residual and spatial consistency approach. Table 1 shows that $\lambda = 1.0$ is the most effective value. Parameters γ and σ are set to 0.7 and 0.3 for Loss function.

Table 1: Comparing the performance for varying λ.

λ	0	0.5	1.0	1.5	2.0	2.5
Accuracy	73.41	75.95	76.42	74.57	72.49	70.52

Performance results when varying the number of training images are presented in Fig.4. To vary the number of training images, we split the training set into 5 random subsets of 5 images per class. Fig.5 shows performance comparison with Recall and Precision curves. We can see that our approach leads to a better detection performance compared with the other algorithms. Fig.6 displays the matching results between the same objects. It can be observed

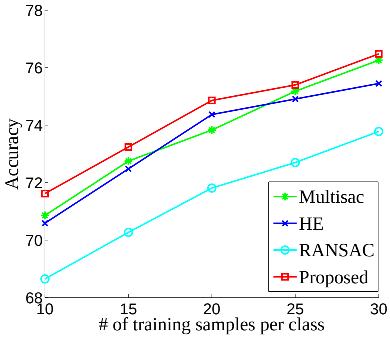

Figure 4: Compare with other method on different training samples per class.

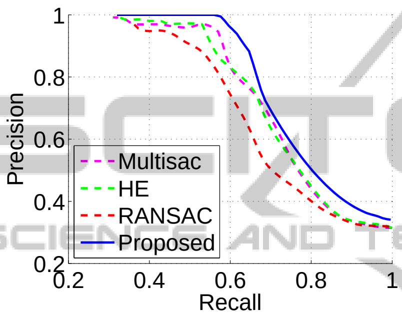

Figure 5: Precision and Recall curve comparison.

that most of matched ones locate on the object. As a reminder, these curves are generated by varying the matching threshold and computing the following values:(TP:True Positive, FP:False Positive, FN:False Negative)

$$
\begin{aligned}
Recall(\%) &= \frac{TP}{TP+FN} \times 100, \\
Precision(\%) &= \frac{TP}{TP+FP} \times 100,
\end{aligned}
\tag{14}
$$

4 CONCLUSIONS

In this paper, we present a new object matching algorithm based on robust estimation of residual consensus and flexible spatial consistency filter. For residual consensus, we model residuals distribution using two-parameter integrated Weibull which is between a power-law and a Gaussian distribution. Then we estimate a series of inlier probabilities, which are updated on the fly. For spatial consistency filter, we measure spatial consistency using geometric relationships of global point distribution in both clockwise and counterclockwise, which is invariant to scale, rotation, and translation especially robust to flipped image. Experiments on clutter background images show that the proposed method leads to improvements in the performance of object detection system.

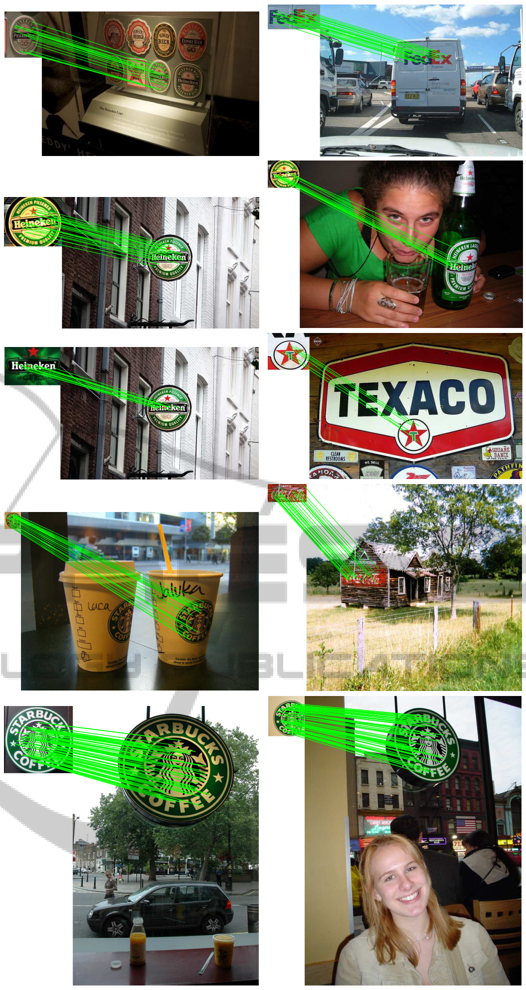

Figure 6: Sample matching results from the same objects.

ACKNOWLEDGEMENTS

This research was supported by the High Technology Research and Development Program of China (2012AA011702, 2011AA01A107).

REFERENCES

Bagdanov, A. D., Ballan, L., Bertini, M., and Del Bimbo, A. (2007). Trademark matching and retrieval in sports video databases. In *Proceedings of the international workshop on Workshop on multimedia information retrieval*, pages 79–86. ACM.

Chin, T.-J., Yu, J., and Suter, D. (2010). Accelerated hypothesis generation for multi-structure robust fitting. In *Computer Vision–ECCV 2010*, pages 533–546. Springer.

Chum, O. and Matas, J. (2005). Matching with prosac-progressive sample consensus. In *Computer Vision and Pattern Recognition, 2005. CVPR 2005. IEEE Computer Society Conference on*, volume 1, pages 220–226. IEEE.

Chum, O., Matas, J., and Kittler, J. (2003). Locally optimized ransac. In *Pattern Recognition*, pages 236–243. Springer.

Comaniciu, D. and Meer, P. (2002). Mean shift: A robust approach toward feature space analysis. *Pattern Analysis and Machine Intelligence, IEEE Transactions on*, 24(5):603–619.

Jegou, H., Douze, M., and Schmid, C. (2008). Hamming embedding and weak geometric consistency for large scale image search. In *Computer Vision–ECCV 2008*, pages 304–317. Springer.

Jiang, Y., Meng, J., and Yuan, J. (2011). Grid-based local feature bundling for efficient object search and localization. In *Image Processing (ICIP), 2011 18th IEEE International Conference on*, pages 113–116. IEEE.

Kalantidis, Y., Pueyo, L. G., Trevisiol, M., van Zwol, R., and Avrithis, Y. (2011). Scalable triangulation-based logo recognition. In *Proceedings of the 1st ACM International Conference on Multimedia Retrieval*, page 20. ACM.

Lazebnik, S., Schmid, C., and Ponce, J. (2006). Beyond bags of features: Spatial pyramid matching for recognizing natural scene categories. In *Computer Vision and Pattern Recognition, 2006 IEEE Computer Society Conference on*, volume 2, pages 2169–2178. IEEE.

Li, T., Mei, T., Kweon, I.-S., and Hua, X.-S. (2011). Contextual bag-of-words for visual categorization. *Circuits and Systems for Video Technology, IEEE Transactions on*, 21(4):381–392.

Lowe, D. G. (2004). Distinctive image features from scale-invariant keypoints. *International journal of computer vision*, 60(2):91–110.

Ni, K., Jin, H., and Dellaert, F. (2009). Groupsac: Efficient consensus in the presence of groupings. In *Computer Vision, 2009 IEEE 12th International Conference on*, pages 2193–2200. IEEE.

Raguram, R., Frahm, J.-M., and Pollefeys, M. (2008). A comparative analysis of ransac techniques leading to adaptive real-time random sample consensus. In *Computer Vision–ECCV 2008*, pages 500–513. Springer.

Russell, B. C., Freeman, W. T., Efros, A. A., Sivic, J., and Zisserman, A. (2006). Using multiple segmentations to discover objects and their extent in image collections. In *Computer Vision and Pattern Recognition, 2006 IEEE Computer Society Conference on*, volume 2, pages 1605–1614. IEEE.

Sattler, T., Leibe, B., and Kobbelt, L. (2009). Scramsac: Improving ransac's efficiency with a spatial consistency filter. In *Computer Vision, 2009 IEEE 12th International Conference on*, pages 2090–2097. IEEE.

Sivic, J. and Zisserman, A. (2003). Video google: A text retrieval approach to object matching in videos. In *Computer Vision, 2003. Proceedings. Ninth IEEE International Conference on*, pages 1470–1477. IEEE.

Sivic, J. and Zisserman, A. (2009). Efficient visual search of videos cast as text retrieval. *Pattern Analysis and Machine Intelligence, IEEE Transactions on*, 31(4):591–606.

Tordoff, B. J. and Murray, D. W. (2005). Guided-mlesac: Faster image transform estimation by using matching priors. *Pattern Analysis and Machine Intelligence, IEEE Transactions on*, 27(10):1523–1535.

Torr, P. H. and Zisserman, A. (2000). Mlesac: A new robust estimator with application to estimating image geometry. *Computer Vision and Image Understanding*, 78(1):138–156.

Wu, Z., Ke, Q., Isard, M., and Sun, J. (2009). Bundling features for large scale partial-duplicate web image search. In *Computer Vision and Pattern Recognition, 2009. CVPR 2009. IEEE Conference on*, pages 25–32. IEEE.

Zhang, Y., Jia, Z., and Chen, T. (2011). Image retrieval with geometry-preserving visual phrases. In *Computer Vision and Pattern Recognition (CVPR), 2011 IEEE Conference on*, pages 809–816. IEEE.